# Infrared photodetachment of $Ce^-$: Threshold spectroscopy and resonance structure

C. W. Walter,* N. D. Gibson,† C. M. Janczak, K. A. Starr, A. P. Snedden, and R. L. Field III
*Department of Physics and Astronomy, Denison University, Granville, Ohio 43023, USA*

P. Andersson
*Department of Physics, Göteborg University, SE-412 96 Göteborg, Sweden*

(Received 19 July 2007; revised manuscript received 19 September 2007; published 7 November 2007; publisher error corrected 9 November 2007)

The negative ion of cerium is investigated using tunable laser photodetachment threshold spectroscopy. The relative cross section for photodetachment from $Ce^-$ is measured over the photon energy range 0.61–0.75 eV using a crossed laser-beam–ion-beam technique. The spectrum of neutral atom production reveals a photodetachment threshold at 0.65 eV, which is interpreted as the threshold for the $Ce^-$ $(4f5d^26s^2\ ^4H_{7/2})$ to Ce $(4f5d6s^2\ ^1G_4)$ ground-state to ground-state transition yielding the electron affinity of Ce to be 0.65(3) eV. At least five narrow peaks are observed in the cross section over the range 0.62–0.70 eV due to negative ion resonances, and their energies and widths are measured. The results are compared to other recent experimental and theoretical studies of $Ce^-$.

DOI: 10.1103/PhysRevA.76.052702 PACS number(s): 32.80.Gc, 32.10.Hq

## I. INTRODUCTION

Investigations of the dynamics of negative ions provide valuable insight into the fundamental problem of many-body motion, which is critical for a detailed understanding of the electronic structure of atoms and molecules. Negative ions provide challenging problems and critical test cases for atomic theory because the added electron is bound to a neutral core; thus, there is no long-range Coulomb binding force. Therefore, the influences of such effects as electron-electron correlation and core polarization are greatly enhanced in negative ions relative to neutral atoms and positive ions. Impressive progress has been made over the past two decades in understanding negative ions through both theoretical and experimental advances; the properties of most atomic negative ions, including their binding energies and electronic structures, are now well established [1–3]. In addition to the properties of ground-state negative ions, there is considerable interest in the excited states of negative ions, including both bound and unbound resonance states [4,5].

Perhaps the most glaring exception to the high-precision information available for the negative ions of most elements remains in the lanthanide atoms [1,2]. The lanthanides are particularly interesting and challenging because the large number of electrons and the presence of several open shells lead to strong valence-valence and core-valence correlation effects. From an experimental standpoint, studies of lanthanide negative ions are challenging because of the difficulty in producing substantial stable beams of the ions [6,7], the need to use less common infrared light sources for threshold investigation due to the small binding energies ($<1$ eV) of the ions, and the possibility of overlapping signals due to multiple bound excited states. These challenges have led to substantial discrepancies between experimental and theoretical determinations of the electron affinities for several of these atoms [2]. Furthermore, even the ground-state configurations of their negative ions have not been firmly established, as the additional electron may enter the open $4f$, $5d$, or $6p$ valence shells.

Of the lanthanides, the negative ion of cerium has received the most theoretical and experimental attention. The ground-state configuration of neutral Ce ($Z=58$) has primary $LS$ character ([Xe] $4f5d6s^2\ ^1G_4^o$) [8]. Early relativistic configuration interaction (RCI) calculations [9] predicted that the ground state of the negative ion would be formed by $6p$ attachment to the neutral ground state. However, more recent larger-scale calculations using the techniques of RCI [10,11] and pseudopotential multireference configuration interaction (MRCI) [12] concluded that the $Ce^-$ ground state is formed by $5d$ attachment, giving a ground-state configuration for the negative ion of primary character ([Xe] $4f5d^26s^2\ ^4H_{7/2}^o$). The binding energy of the ground state of $Ce^-$, corresponding to the electron affinity of Ce, was calculated to be 0.428 eV by O'Malley and Beck [10] and 0.58(10) eV by Cao and Dolg [12]. A later calculation by O'Malley and Beck [11] with a larger basis set yielded an electron affinity of 0.511 eV, but the authors note that test calculations suggested that more binding would be obtained through inclusion of opening of the $5p$ subshell.

$Ce^-$ has been investigated in several experiments over the past 14 years. In 1993, Garwan *et al.* [13] estimated the electron affinity to be $\geq 0.6$ eV based on the relative yield of $Ce^-$ from a sputtering source in accelerator mass spectrometry experiments. They also suggested the possibility that $Ce^-$ may have multiple bound excited states. Subsequently, in 1997, Berkovits *et al.* [14] observed two sharp increases in a coarsely stepped $Ce^-$ photodetachment cross-section spectrum at photon energies of 2.130 eV and 2.165 eV, which were interpreted as opening thresholds for detachment to excited states of Ce. Their interpretation of the spectrum led to an electron affinity of 0.700(10) eV. However, that value is questionable because it was based on the assumption of $6p$ attachment for the ground state of the negative ion, which is not consistent with more recent theoretical results that indicate $5d$ attachment [10–12].

*walter@denison.edu
†gibson@denison.edu

 

The first detailed photodetachment study of $Ce^-$ was done by Davis and Thompson in 2002 [15]. They used laser photoelectron spectroscopy (LPES) to measure the kinetic energies of electrons detached from $Ce^-$ at two fixed laser wavelengths (1064 nm and 514.5 nm). The photoelectron spectrum at 514.5 nm showed three prominent peaks, the largest of which, also at the highest electron energy, was interpreted as due to the ground-state negative ion to ground-state neutral atom transition. Based on this interpretation, the electron affinity of Ce was determined to be 0.955(26) eV and at least two bound excited states of $Ce^-$ were identified with binding energies of 0.921(25) eV and 0.819(27) eV relative to the Ce ground state.

Very recently, O'Malley and Beck [11] have reinterpreted the LPES data of Davis and Thompson [15] based on calculations of the partial photodetachment cross sections from the collection of $Ce^-$ bound states to various Ce states. Their calculations indicated that the cross section for photodetachment from ground-state $Ce^-$ to ground-state Ce is very weak compared to the cross sections for transitions to several excited states of the neutral atom due to the differing electronic configurations. Therefore, the strongest peaks in the LPES data were reinterpreted as due to detachment to excited states of Ce, thus reducing the inferred binding energy of the negative ion. This reinterpretation leads to an electron affinity of 0.660 eV [11], which is substantially lower than the original LPES value [15], but consistent with previous *ab initio* theoretical values [10,12].

In the present study, we have performed a detailed tunable laser photodetachment threshold spectroscopy investigation of $Ce^-$. The relative photodetachment cross section was measured over the photon energy range 0.61–0.75 eV, revealing a characteristic *p*-wave threshold near 0.65 eV. This threshold is interpreted as the ground-state $Ce^-$ to ground-state Ce transition, yielding the electron affinity of Ce to be 0.65(3) eV, consistent with the semiempirical results of O'Malley and Beck [11] and the *ab initio* calculations of Cao and Dolg [12]. In addition to the threshold behavior, the cross section shows at least five narrow peaks over this energy range that are associated with excitation from the $Ce^-$ target ion to excited states of the negative ion followed by autodetachment or photodetachment by absorption of a second photon.

## II. EXPERIMENTAL METHOD

In the present study, the relative cross section for photodetachment from negative ions was measured as a function of photon energy using a crossed ion-beam–laser-beam system. Negative ions produced by a cesium sputtering source (NEC SNICS II) were accelerated to 13 keV and mass selected using a 90° focusing sector magnet. Sets of electrostatic lenses and vertical and horizontal deflection plates before and after the magnet were used to collimate and steer the beam into a UHV interaction chamber. Beam profile monitors (NEC model BPM80) situated before and after the magnet provided real-time information on the beam shape and position. In the interaction region, the ion beam was intersected perpendicularly by a pulsed laser beam. Following the interaction region, residual negative ions in the beam were electrostatically deflected into a Faraday cup to monitor the ion current. Neutral atoms continued undeflected to strike a multidynode electron multiplier detector (ETP model 14150H). The production of neutral atoms by stripping collisions with background gas was small due to the low pressure in the interaction chamber ($\sim 8 \times 10^{-10}$ torr) and was accounted for in the analysis, as described below.

The detector was operated in analog mode, and the voltage output was recorded as a function of time after each laser pulse using a digital storage oscilloscope (LeCroy model LT364). The oscilloscope functioned effectively as a gated integrator and boxcar averager. At each wavelength setting, the signal from 400–800 laser shots was averaged and the voltage was integrated over the arrival window corresponding to the flight time of Ce atoms from the interaction region to the detector. The average background voltage was subtracted from this integrated voltage to obtain a signal proportional to the number of neutral atoms produced by each laser pulse. This signal was then normalized to the ion beam current and the average laser photon flux at each wavelength to obtain the relative cross section for photodetachment. A LabVIEW computer program was used to control the laser wavelength, monitor the beam current and laser power, and interface with the oscilloscope. The spectra were built up by repeatedly scanning over the photon energy range of interest and averaging the resulting individual scans.

The laser system consisted of a tunable optical parametric oscillator (OPO) (Lambda Physik ScanMate OPPO) pumped by a pulsed Nd:YAG laser (Coherent Infinity) operating at 50 Hz. The tripled output of the Nd:YAG laser at 355 nm was used to pump an integrated dye laser and OPO crystal system. The OPO produced visible "signal" light over the range 410–710 nm and infrared "idler" light over the range 710–2500 nm. The dye laser output was used to seed the OPO at the visible signal wavelength in order to narrow its bandwidth to approximately 0.12–0.15 $cm^{-1}$. The signal and idler beams were separated by a combination of optical alignment and glass absorption filters. The linearly polarized light entered and exited the interaction chamber through windows (7056 glass) mounted at Brewster's angle. The energy per laser pulse measured through the interaction region was typically in the range 0.03–0.1 mJ with pulse duration 2.5 ns. The wavelength of the visible signal light was measured with a pulsed wavemeter (Burleigh model WA-4500). The photon energy of the infrared idler light was then calculated based on conservation of energy by subtracting the measured visible photon energy from the photon energy of the tripled Nd:YAG fundamental [3.494 33(1) eV [16]].

The production of beams of lanthanide negative ions using a standard sputtering source is problematic because lanthanides coat the ionizer and reduce its efficiency due to their low work functions. This leads to relatively weak, unstable ion beams that have a short life of only a few hours before maintenance of the source is required [6]. To address this problem, a modified double-layer cathode design, developed by Saitoh *et al.* [7], was used in the present experiments. A copper cathode was first packed with cerium oxide ($CeO_2$) powder and then covered by a layer of tungsten powder 2 mm thick. A 1-mm-diam hole was then drilled through the tungsten, creating a channel for sputtering of the $CeO_2$. This channel limited the solid angle for the directions of sputtered

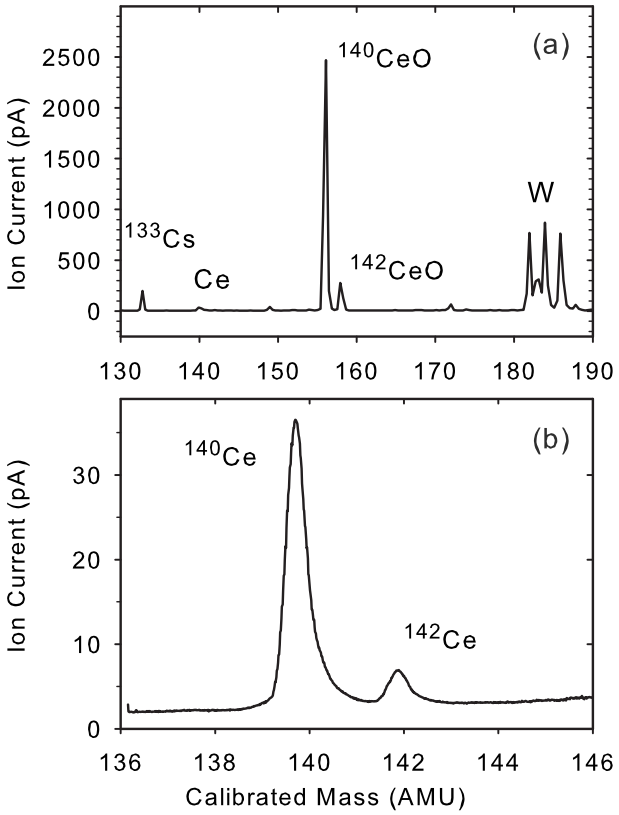


FIG. 1. (a) Negative ion mass spectrum obtained with a double-layer $CeO_2$+W cathode in the sputtering source. The mass scale was calibrated using the peaks of $Cs^-$ (133 amu), $^{140}CeO^-$ (156 amu), and $W^-$ isotopes (182, 183, 184, and 186 amu). (b) Expanded view of the $Ce^-$ region of the mass spectrum, showing the two isotopes of Ce (140, 142 amu). Note the slight tails on the high-mass sides of the peaks due to small amounts of the hydride ions $CeH^-$.

ions leaving the cathode, thus reducing the coverage of the ionizer by the cerium compounds. In addition, sputtered tungsten ions continuously coated the ionizer to prevent buildup of a poisoning cerium layer. Using this cathode design, the source produced beams that were stable for up to 48 h with typical currents through the interaction region of 30–100 pA.

The ion mass spectrum obtained with a $CeO_2$ cathode is shown in Fig. 1. The mass scale was calibrated using the peaks of $Cs^-$ (mass 133 amu) and $^{140}CeO^-$ (156 amu) and the isotopes of $W^-$ (182–186 amu). The mass resolution of the system was determined to be $\Delta m/m \approx 1/240$; this high mass resolution was necessary to reject possible molecular contaminants in the beam, as discussed below. The dominant cerium compound in the beam was measured to be $CeO^-$, which is consistent with previous observations for a cerium oxide cathode [6,7]. The two primary isotopes of Ce, masses 140 amu and 142 amu, were well separated in the mass spectrum. The isotope percentages were measured to be $^{140}Ce:{}^{142}Ce = 88\%:12\%$, in excellent agreement with the natural abundances of 89%:11%. The photodetachment studies reported here were performed on the more abundant mass 140 amu isotope.

Careful tests were performed to rule out possible contributions from the hydride ion $CeH^-$ to the measured $Ce^-$ photodetachment spectrum. Figure 1(b) shows that the $^{140}Ce^-$ and $^{142}Ce^-$ mass peaks have slight tails on the high-mass side that may be due to a very small amount of $CeH^-$ in the beam; these tails are slightly more pronounced for $Ce^-$ than for other mass peaks. The high mass resolution of the system greatly reduces the overlap of the peaks, separated by 1 amu. Gaussian fits to the measured mass spectrum determined that the $CeH^-$ contribution was less than 0.1% of the ion current at the maximum of the $^{140}Ce^-$ peak. However, even such a small contaminant may produce significant photodetachment signal if the cross section is large; therefore, further tests were made to confirm that $CeH^-$ does not affect the present results. The photodetachment signal was measured with the magnetic field set halfway down the $Ce^-$ mass peak on both the low-mass and high-mass sides, and compared to the signal at the maximum of the $Ce^-$ peak. This test was performed at photon energies of 0.6981 eV (at the center of peak *E*; see below) and 0.6983 eV (in the continuum above peak *E*). The measured signal normalized to ion current was the same within statistical uncertainties for the three mass settings at each photon energy. Thus, $CeH^-$ is not a significant source of contamination in the present measurements.

As a final test of the experimental system, the spectrum for photodetachment from the negative ion of platinum was measured near the ground-state $Pt^-$ to ground-state Pt threshold. The fit of a Wigner *p*-wave threshold curve [see Eq. (1) below] to our measured cross-section data yielded a threshold energy of 2.125 12(9) eV, corresponding to the electron affinity of Pt. Our value is in excellent agreement with the accepted value for the electron affinity of Pt of 2.125 10(5) eV measured by Bilodeau *et al.* [17], confirming the performance of our experimental system.

## III. RESULTS AND DISCUSSION

The measured relative photodetachment cross section from $Ce^-$ over the photon energy range 0.61–0.75 eV is shown in Fig. 2. This spectrum was taken with the infrared idler beam from the seeded, narrow-band OPO. Two different laser dyes were used to seed the OPO at the visible complement wavelength over this range; Exalite 428 (Exciton) to produce 0.614–0.653 eV and Coumarin 450 (Exciton) to produce 0.635–0.752 eV. The two scans were normalized over the overlapping range, requiring a 14% change in the relative magnitudes; this small difference was likely due to changes in the laser beam spatial profile between the two dyes.

The spectrum of Fig. 2 consists of a slowly varying continuum component with at least five prominent peaks superimposed. The base-line signal over the range 0.61–0.65 eV is likely due to photodetachment from bound excited states of $Ce^-$ in the beam, with binding energies less than 0.60 eV. The gradual increase in the cross section beginning near 0.65 eV may be due to the opening of the ground-state $Ce^-$ to ground-state Ce detachment channel. The five narrow peaks in the spectrum, labeled *A*–*E*, are due to transitions to excited states of the negative ion prior to detachment, leading to an increased cross section relative to the direct detach-

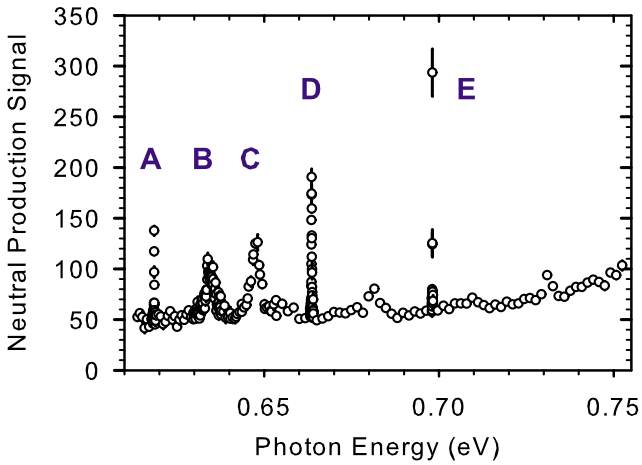


FIG. 2. (Color online) Measured normalized neutral production signal (arbitrary units) for photodetachment from $Ce^-$ obtained as the average of multiple sweeps over the entire threshold region. Five resonance peaks are labeled *A*—*E*. Finely stepped spectra separately measured over peaks *A*, *B*, *D*, and *E* are included with the coarsely stepped spectrum. Error bars are one standard deviation of the mean of the individual signals for the multiple sweeps at each photon energy.

ment processes responsible for the smoothly varying continuum. Two additional peaks may be observed in the less pronounced structures near 0.68 eV and 0.73 eV. It should be noted that there may be additional narrow peaks in the present energy range that were not detected because of the coarse steps used in the scans of Fig. 2. Higher-resolution spectra of the five labeled individual peaks are shown in Figs. 3 and 4. Note that in Fig. 2, these high-resolution spectra for peaks *A*, *B*, *D*, and *E* have been added to the spectrum acquired by scanning with coarser steps over the longer range shown. A shift in the signal scale of~25% for peak *E* was required to match the coarse spectrum, but the other peaks were not shifted.

Interpretation of the photodetachment spectrum is complicated by several factors. First, $Ce^-$ is likely to have multiple bound excited states [9–13,15], possibly of both odd parity ($5d$ attachment) and even parity ($6p$ attachment), so that the target ions are likely to have a range of initial excitation energies and electronic configurations. Furthermore, photodetachment from these excited ions produces significant background signal at photon energies below the $Ce^-$ ground-state threshold energy. A second complicating factor is that neutral Ce has many low-lying excited states, leading to a potentially large number of opening detachment thresholds. Finally, interpretation is complicated by the substantial discrepancies in the available values for the electron affinity of Ce, ranging from 0.58(10) eV to 0.66 eV from theoretical and semiempirical calculations [11,12] to 0.955(26) eV from experiment [15]. We will first consider the threshold behavior, followed by analysis and discussion of the resonance structure.

### A. Threshold

A consistent interpretation of the spectrum is that the increase in the continuum cross section over the energy range

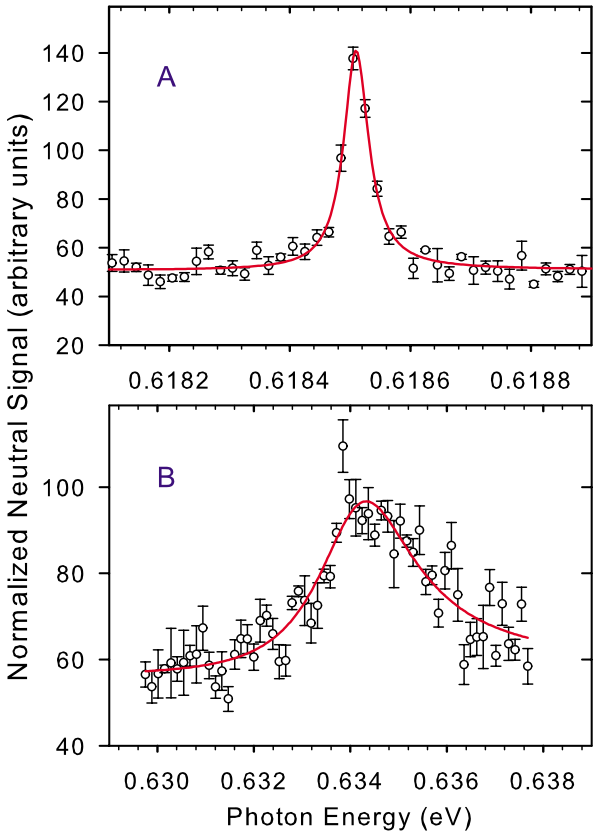


FIG. 3. (Color online) Measured normalized neutral production signal for photodetachment from $Ce^-$ in the vicinity of peaks *A* and *B* (see Fig. 2). Open circles, measured data; solid line, fit of the Fano function [Eq. (2)] to the data. Note the change in photon energy scale between the graphs.

0.61–0.75 eV (see Fig. 2) is due to the opening of the ground-state $Ce^-$ to ground-state Ce detachment channel. The photodetachment cross section above an opening threshold is given by the Wigner threshold law [18]

$$\sigma = \sigma_0 + a(E - E_0)^{\ell+1/2}, \tag{1}$$

where $E$ is the photon energy, $E_0$ is the threshold energy, $\ell$ is the angular momentum of the departing electron, $a$ is a scaling constant, and $\sigma_0$ is the background cross section (assumed constant for $Ce^-$ here). The flat base line from 0.61 to 0.65 eV followed by a gradual increase in the continuum portion of the cross section is consistent with the shape of a $p$-wave ($\ell=1$) threshold. Attempts to fit the data in this range with the Wigner law [Eq. (1)] in order to determine the threshold energy and angular momentum were inconclusive due both to the superimposed resonance peaks, which obscure the continuum behavior, and to the statistical scatter in the data. The signal-to-noise ratio is adversely affected both by experimental factors, including the low ion current characteristic of lanthanides and the instability of the laser operating near the long-wavelength end of its tuning range and by the weakness of this opening channel relative to the background cross section (this aspect is discussed further below).

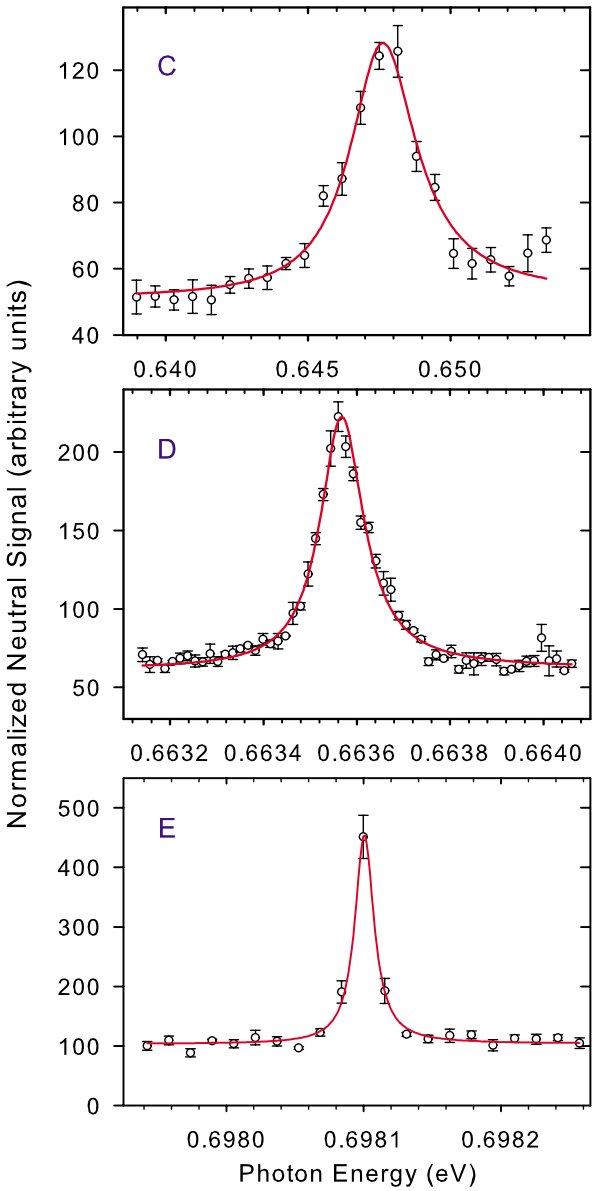


FIG. 4. (Color online) Measured normalized neutral production signal for photodetachment from $Ce^-$ in the vicinity of peaks *C*, *D*, and *E* (see Fig. 2). Open circles, measured data; solid line, fit of the Fano function [Eq. (2)] to the data. Note the change in photon energy scale between the graphs.

Because of the difficulties in directly fitting the continuum component of the measured spectrum, a different approach was followed using a simulated threshold spectrum based on the recent results of O'Malley and Beck [11]. Those authors used theoretical calculations of electronic structure and photodetachment partial cross sections to reanalyze the LPES data of Davis and Thompson [15], yielding an electron affinity of 0.660 eV and a $Ce^-$ ground-state configuration of $(4f5d^26s^2\ ^4H_{7/2})$. This would lead to a threshold at 0.660 eV for the $Ce^-$ ground-state to Ce $(4f5d6s^2\ ^1G_4)$ ground-state detachment channel, through removal of a $5d$ electron. Detachment of a *d* electron can produce a *p*- or *f*-wave free electron, with the *p*-wave detachment channel being strongly dominant near threshold.

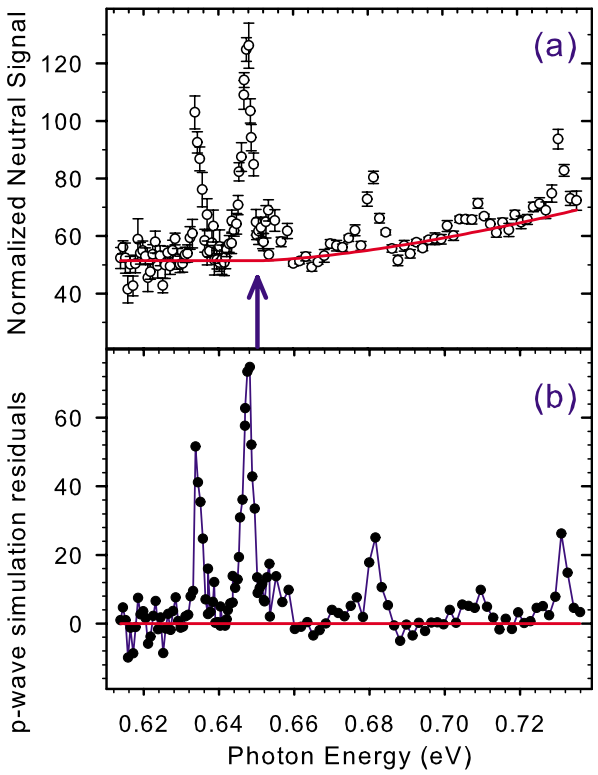


FIG. 5. (Color online) (a) Relative cross section (arbitrary units) for photodetachment from $Ce^-$ in the near-threshold region. Open circles, measured data; heavy solid line (red), simulated *p*-wave Wigner threshold curve [Eq. (1)] with fixed threshold energy of 0.65 eV indicated by the vertical arrow. For the *p*-wave curve, only the scaling factor *a* was adjusted. (b) Residual differences between the data and the simulated curve. The large peaks at 0.634 eV and 0.648 eV are resonance peaks *B* and *C*, respectively. Additional smaller resonance peaks are at 0.68 eV and 0.73 eV.

To test the interpretation of the observed threshold as the $Ce^-$ $(4f5d^26s^2\ ^4H_{7/2})$ to Ce $(4f5d6s^2\ ^1G_4)$ ground-state to ground-state transition, a simulated continuum spectrum was calculated using the Wigner threshold law [Eq. (1)] assuming a fixed threshold energy and $\ell=1$ for *p*-wave detachment. The background cross section $\sigma_0$ was fixed at the average of the measured cross section over the low-energy range 0.614–0.630 eV; the continuum cross section is constant within the uncertainties of the data points over this range. The only adjustable parameter was then the amplitude constant *a*, which was varied to yield the best visual match to the continuum component of the measured cross section between the threshold and 0.736 eV. The simulation procedure was then repeated with different values for the threshold energy to determine the range of threshold energies that were consistent with the data. This process yielded a value for the threshold of 0.65(3) eV. The optimal simulated threshold curve is shown together with the measured cross section in Fig. 5(a), and the residual differences between the data and the simulated curve are shown in Fig. 5(b). The residuals show very good agreement for the continuum component of the spectrum and clearly display the superimposed resonance peaks, including the prominent peaks *B* and *C*, as well as the

weaker resonance peaks near 0.68 eV and 0.73 eV. Note that peaks *A*, *D*, and *E* are not visible in the spectrum of Fig. 5, because those narrow peaks lie between steps of the photon energy for these coarse scans.

The simulated threshold curve provides a very good representation of the measured continuum cross section, with a flat base line from 0.61 to 0.65 eV followed by a gradually increasing slope above 0.65 eV characteristic of a *p*-wave threshold. The measured cross section returns to the baseline value (~51) in between peaks *B* and *C* and near 0.65 eV at the end of the tail of peak *C*, before increasing by a factor of ~40% over the next 90 meV, in good agreement with the simulated curve. Above the energy range shown in Fig. 5, the data begin to increase more rapidly than the *p*-wave curve; this deviation from Wigner law behavior is to be expected as the energy is increased out of the near-threshold region [19,20]. It would be possible to improve the agreement in this higher-energy region by including an *f*-wave component in the simulated curve; however, the important result is that the simulation works very well with only a single adjustable parameter, the scaling constant *a*. The deviation from *p*-wave behavior above 0.74 eV may also be due to the opening of a new channel for detachment from the $Ce^-$ to an excited state of Ce.

Given the signal to noise of the present data and the complications due to overlapping resonance peaks, we recommend a value of 0.65(3) eV for the electron affinity based on the measured threshold photodetachment spectrum. The very good agreement between the measured spectrum and the simulated *p*-wave threshold behavior gives strong support for the electron affinity of 0.660 eV determined by O'Malley and Beck [11] and for their calculated ground-state configuration of $Ce^-$ as $(4f5d^26s^2\ ^4H_{7/2})$. The present results also agree well with the theoretical calculations of Cao and Dolg [12], which yielded an electron affinity of 0.58(10) eV with the same ground-state configuration. However, this electron affinity is substantially lower than the experimental value of 0.955(26) eV determined by Davis and Thompson using LPES [15].

The relative weakness of the ground-state negative ion to ground-state neutral atom channel observed in the present measured spectrum can be understood based on the relevant electronic configurations. As first discussed by O'Malley and Beck [11], transition from the $Ce^-$ ground state $(4f5d^26s^2\ ^4H_{7/2})$ to the neutral ground state $(4f5d6s^2\ ^1G_4)+\varepsilon p$, $\varepsilon f$ is spin forbidden for the dominant *LS* terms. Therefore, the ground-state threshold shows a gradual turn-on relative to the substantial background cross section from photodetachment of excited ions in the beam, and photodetachment to excited states of Ce may be significantly stronger than to the ground-state. This consideration led to O'Malley and Beck's [11] reinterpretation of the Davis-Thompson LPES data [15], reducing the inferred electron affinity by three-tenths of an eV to 0.660 eV.

The possibility must be considered that the observed threshold near 0.65 eV may be due to photodetachment from excited states of $Ce^-$, rather than from the ground state. O'Malley and Beck's calculations [11] predict the existence of over 20 bound states of $Ce^-$, with the first excited state $(4f5d^26s^2\ ^4H_{9/2})$ being bound by 0.550 eV, which is 0.110 eV above the $^4H_{7/2}$ $Ce^-$ ground state. Given the high temperature of the sputtering source, estimated to be ~1500 K [6], a substantial range of excited states should be produced in the source. Many of these excited ions, especially those of odd parity with longer lifetimes, would likely survive the ~33 $\mu$s flight time from the source to the interaction region and would thus be potential targets for photodetachment. However, the photodetachment partial cross-section calculations [11] indicate no significant structure due to photodetachment from low-lying excited states (bound by >0.3 eV) at photon energies over the range in the present study of 0.61–0.75 eV. Furthermore, the increase in the continuum cross section by a factor of ~40% over the first 90 meV above the threshold at 0.65 eV indicates that the target ion state must have a substantial population in the beam; therefore, it is unlikely that this structure is due to photodetachment from high-lying bound states which would be expected to comprise only a small fraction of the beam.

TABLE I. Resonance parameters for peaks measured in photodetachment from $Ce^-$ obtained from fits of the Fano resonance formula [Eq. (2)] to the measured data. Relative amplitude is the amplitude of the peak above the baseline divided by the amplitude of peak *D* for comparison of relative strengths.

| Peak | Energy $E_r$ (meV) | Width $\Gamma$ (meV) | Line shape $q$ | Rel. amp. |
|---|---|---|---|---|
| *A* | 618.5(2) | 0.050(4) | 58(65) | 0.6 |
| *B* | 634.2(3) | 2.5(5) | 7(3) | 0.3 |
| *C* | 647.6(3) | 2.8(3) | 27(27) | 0.5 |
| *D* | 663.6(2) | 0.114(7) | 53(48) | 1 |
| *E* | 698.1(2) | 0.017(4) | 100(170) | 2.3 |

### B. Resonances

We turn now from the threshold structure to analysis and interpretation of the observed narrow peaks *A*–*E* (see Figs. 3 and 4). To determine the resonance characteristics, Fano profiles [21] were fit to the peaks. The Fano formula gives the cross section in the vicinity of the peak as

$$\sigma = \sigma_0 + b\frac{(q+\varepsilon)^2}{1+\varepsilon^2}, \tag{2}$$

where $\sigma_0$ is the continuum cross section (assumed constant over the narrow energy range of the peak in the present case), $q$ is the line-shape parameter, and $b$ is a scaling constant. The factor $\varepsilon$ is given by $(E-E_r)/(\Gamma/2)$, where $E$ is the photon energy, $E_r$ is the energy of the resonance, and $\Gamma$ is the peak width (dependent on the lifetime of the excited state). The resonance energies, widths, and other properties obtained from fitting Eq. (2) to the measured peaks are listed in Table I. The fitted curves are included with the data in Figs. 3 and 4. Note that two weaker peaks near 0.68 eV and 0.73 eV are also observed in the spectrum of Fig. 2 in addition to the labeled peaks *A*–*E* that have been investigated in detail. The uncertainties in Table I are given as one standard deviation (1-SD) of the uncertainties of the fitting param-

eters; for the resonance energies, the fitting uncertainty is added in quadrature with the 1-SD uncertainty in the absolute photon energy calibration. The large uncertainties in the fitted line-shape parameters $q$ are due to the high correlation between $q$ and the scaling constant $b$ when the value of $q$ is large, as is the case for the present peaks.

The narrowest of the observed peaks, peak $E$, is significantly instrumentally broadened. The measured peak width of 0.017 meV (0.13 $cm^{-1}$) is comparable to the bandwidth of the laser, 0.015–0.019 meV (~0.12–0.15 $cm^{-1}$); therefore, the natural width of peak $E$ may be substantially smaller than the measured value. Peak $A$ is slightly instrumentally broadened; subtracting in quadrature the laser bandwidth from the measured peak width reduces the width by about 10%, yielding a natural width of 0.046 meV for peak $A$. The other peaks, being substantially wider, are not significantly broadened by the laser bandwidth.

While the Fano function [Eq. (2)] provides a very good representation for the peaks, the fairly large values for the line-shape parameters for all of the peaks except peak $B$ indicate that those peaks are quite symmetric; therefore, simple Lorentzians provide adequate representations of the data for those peaks. Indeed, the resonance energies and widths determined by Lorentzian fits to the data are within the quoted uncertainties of the values obtained with Fano fits for all of the peaks except peak $B$. In contrast, the asymmetric shape of peak $B$ leads to the relatively small value of $q=7$ for its line-shape parameter and to noticeable differences between the Fano and Lorentz fits. The unusual shape of this peak suggests that it may be composed of at least two unresolved peaks, with the lower-energy component being somewhat narrower than the broader higher-energy peak. Also, note that there is possible additional structure on the high-energy tail of peak $C$.

Peaks in photodetachment spectra generally arise from photoexcitation of unbound excited states of the negative ion. Traditionally, these autodetaching excited states are classified as being either Feshbach or shape resonances [3]. Feshbach resonances lie energetically below the parent state of the neutral atom; therefore, they usually have longer autodetachment lifetimes than shape resonances (which lie above the parent state), and thus Feshbach resonances are generally narrower in width than shape resonances.

It is also possible to photoexcite from a low-lying bound state to a high-lying bound state of a negative ion. Such a state cannot autodetach because it lies energetically below the ground state; however, it can subsequently absorb an additional photon to provide the energy necessary to detach an electron. Bound-bound transitions have been studied using multiphoton techniques for $E2$ and $M1$ transitions in a variety of negative ions; see the reviews in [1,2,22]. In contrast, only one negative ion, $Os^-$, has been experimentally demonstrated to have bound states of opposite parity so that an electric-dipole $E1$ transition is allowed between bound states [23].

Clearly, the nature of the states responsible for the observed peaks in the present measurements depends crucially on the positioning of the photoexcited $Ce^-$ states relative to the Ce ground state. The uncertainty range of the ground-state threshold energy of 0.65(3) eV encompasses the range of the observed peaks (with the exception of peak $E$), so unique identification is not possible based on the present data alone. All of the peaks may be due to shape and/or Feshbach resonances above the Ce ground state that are excited from the $Ce^-$ ground state. A second possible interpretation is that peaks $A$, $B$, and $C$ are below the ground-state threshold, while peaks $D$ and $E$ are above threshold. In this second scenario, peak $D$ at 0.6636 eV would likely be a $p$-wave shape resonance slightly above threshold; similar resonances have been observed in a number of ions, including valence-shell photodetachment from $He^-$ [24,25], $Cs^-$ [26], $Ca^-$ [27], and $Os^-$ [23] and inner-shell photodetachment from $C^-$ [28,29] and $B^-$ [30,31]. The measured width of peak $D$ [0.114(7) meV] is somewhat narrower than the shape resonances observed in other ions, ranging in width from 0.438 meV for $Os^-$ [23] to 34.6 meV for $Ca^-$ [27]. The peak width for a shape resonance should be narrower the closer the resonance is to threshold, so that peak $D$ may lie just above the ground-state threshold. In contrast, peak $E$ is more than a factor of 10 narrower than peak $D$, making it likely that this peak is due to a Feshbach resonance.

If peaks $A$, $B$, and $C$ lie in energy below the ground-state threshold, then they may be due to excitation of bound states of $Ce^-$, rather than unbound resonances. The measured signal on these peaks would then be due to a resonant two-step detachment process: weakly bound $Ce^-$ excited states are initially excited from the $Ce^-$ ground state by absorption of one photon followed by absorption of a second photon, causing detachment from the excited ion. A similar process led to the observation of the bound-bound transition in $Os^-$ [23]. The calculations of O'Malley and Beck [11] predict three bound states of $Ce^-$ with even parity ($6p$ attachment) to lie within 83 meV of the neutral ground state, while the calculations of Cao and Dolg [12] show two such states in this region. The $E1$ $f$ values are substantial for some of the possible transitions to these even-parity states from the odd-parity $Ce^-$ ground state [11], raising the possibility that one or more of peaks $A$, $B$, or $C$ could be the result of electric-dipole-allowed transitions. Note, for example, that the measured energy of peak $A$ (0.6185 eV) is very close to the excitation energy of the $Ce^-$ ($4f5d^26s^2 6p\ ^4I^e_{9/2}$) bound state from the ($4f5d^26s^2\ ^4H^o_{7/2}$) ground state, which is calculated to be 0.615 eV by O'Malley and Beck [11]. However, the uncertainties in the energies of both the $Ce^-$ ground-state and excited-state energies in the experiments and theoretical calculations preclude a unique identification of the observed peaks at present.

## IV. CONCLUSIONS

The present results provide a detailed threshold photodetachment spectrum for a lanthanide negative ion and reveal rich resonance structure near threshold. The measured photodetachment cross section from $Ce^-$ shows a $p$-wave threshold near 0.65 eV, which is interpreted as the threshold for the $Ce^-$ ($4f5d^26s^2\ ^4H_{7/2}$) to Ce ($4f5d6s^2\ ^1G_4$) ground-state to ground-state transition. This threshold energy yields a recommended value of 0.65(3) eV for the electron affinity of Ce, which is in very good agreement with the semiempirical

results of O'Malley and Beck [11] and the theoretical calculations of Cao and Dolg [12]. Future experiments at lower photon energies will be useful to search for photodetachment thresholds from the low-lying excited states of $Ce^-$, in particular the $^4H_{9/2}$ state predicted to be bound by 0.550 eV [11].

At least five resonance peaks have been observed and the energies and widths of the peaks measured. One or more of these peaks may be due to bound-bound $E1$ transitions in the negative ion, making $Ce^-$ a good candidate for further study as possibly only the second example of a negative ion with bound states of opposite parity for which electric-dipole transitions are allowed. The nature of the excited states of $Ce^-$ will be further investigated in future experiments by measuring the laser pulse energy dependence of the neutral atom signal to determine whether the peaks are due to one- or two-photon processes.

The present study of $Ce^-$ is the first in a planned series of experiments to apply threshold photodetachment spectroscopy to investigate other lanthanide negative ions. Substantial progress has been made in photoelectron spectroscopy of a number of these ions by Davis, Thompson, and Covington [32], but some significant puzzles still remain [33]. Full understanding of the complexities of $Ce^-$ and other lanthanide negative ions may require the use of additional techniques, such as state-selective product atom detection [2,34], tunable photodetachment combined with photoelectron spectroscopy [35], and/or further theoretical calculations of energy-dependent cross sections for relevant photodetachment channels and resonance structure.

## ACKNOWLEDGMENTS

We thank S. M. O'Malley, D. R. Beck, and R. C. Bilodeau for helpful discussions. We thank Ken Bixler, Dave Richardson, Craig Mosier, and Jacob Shapiro for technical assistance. This material is based in part upon work supported by the National Science Foundation under Grants Nos. 0140233 and 0456916. C.M.J., K.A.S., A.P.S., and R.L.F. received partial support from Denison University's Anderson Summer Research Fund, and P.A. received partial support from the Swedish Research Council and Mary von Sydow's donations fund.

[1] T. Andersen, H. K. Haugen, and H. Hotop, J. Phys. Chem. Ref. Data **28**, 1511 (1999).
[2] T. Andersen, Phys. Rep. **394**, 157 (2004).
[3] D. J. Pegg, Rep. Prog. Phys. **67**, 857 (2004).
[4] S. J. Buckman and C. W. Clark, Rev. Mod. Phys. **66**, 539 (1994).
[5] V. K. Ivanov, J. Phys. B **32**, R67 (1999).
[6] R. Middleton, *A Negative-Ion Cookbook* (University of Pennsylvania, Philadelphia, 1990).
[7] Y. Saitoh, B. Yotsombat, K. Mizuhashi, and S. Tajima, Rev. Sci. Instrum. **71**, 955 (2000).
[8] *Atomic Energy Levels—The Rare-Earth Elements*, edited by W. C. Martin, R. Zalubas, and L. Hagan, Natl. Bur. Stand. Ref. Data Ser., Natl. Bur. Stand. (U.S.) Circ. No. 60 (U.S. GPO, Washington, D.C., 1978).
[9] K. Dinov, D. R. Beck, and D. Datta, Phys. Rev. A **50**, 1144 (1994).
[10] S. M. O'Malley and D. R. Beck, Phys. Rev. A **61**, 034501 (2000).
[11] S. M. O'Malley and D. R. Beck, Phys. Rev. A **74**, 042509 (2006).
[12] X. Cao and M. Dolg, Phys. Rev. A **69**, 042508 (2004).
[13] M. Garwan, A. E. Litherland, M. Nadeau, and X. Zhao, Nucl. Instrum. Methods Phys. Res. B **79**, 631 (1993).
[14] D. Berkovits, S. Ghelberg, O. Heber, and M. Paul, Nucl. Instrum. Methods Phys. Res. B **123**, 515 (1997).
[15] V. T. Davis and J. S. Thompson, Phys. Rev. Lett. **88**, 073003 (2002).
[16] H. H. Andersen, P. Balling, P. Kristensen, U. V. Pedersen, S. A. Aseyev, V. V. Petrunin, and T. Andersen, Phys. Rev. Lett. **79**, 4770 (1997).
[17] R. C. Bilodeau, M. Scheer, H. K. Haugen, and R. L. Brooks, Phys. Rev. A **61**, 012505 (1999).
[18] E. P. Wigner, Phys. Rev. **73**, 1002 (1948).
[19] T. F. O'Malley, Phys. Rev. **137**, A1668 (1965).
[20] J. W. Farley, Phys. Rev. A **40**, 6286 (1989).
[21] U. Fano, Phys. Rev. **124**, 1866 (1961).
[22] R. C. Bilodeau and H. K. Haugen, in *Photonic, Electronic, and Atomic Collisions, Proceedings of XXII International Conference, Santa Fe, 2001*, edited by J. Burgdorfer, J. S. Cohen, S. Datz, and C. R. Vane (Rinton Press, Princeton, 2002), p. 127.
[23] R. C. Bilodeau and H. K. Haugen, Phys. Rev. Lett. **85**, 534 (2000).
[24] J. R. Peterson, Y. K. Bae, and D. L. Huestis, Phys. Rev. Lett. **55**, 692 (1985).
[25] C. W. Walter, J. A. Seifert, and J. R. Peterson, Phys. Rev. A **50**, 2257 (1994).
[26] M. Scheer, J. Thogersen, R. C. Bilodeau, C. A. Brodie, H. K. Haugen, H. H. Andersen, P. Kristensen, and T. Andersen, Phys. Rev. Lett. **80**, 684 (1998).
[27] C. W. Walter and J. R. Peterson, Phys. Rev. Lett. **68**, 2281 (1992).
[28] N. D. Gibson, C. W. Walter, O. Zatsarinny, T. W. Gorczyca, G. D. Akerman, J. D. Bozek, M. Martins, B. M. McLaughlin, and N. Berrah, Phys. Rev. A **67**, 030703(R) (2003).
[29] C. W. Walter, N. D. Gibson, R. C. Bilodeau, N. Berrah, J. D. Bozek, G. D. Ackerman, and A. Aguilar, Phys. Rev. A **73**, 062702 (2006).
[30] T. W. Gorczyca, Radiat. Phys. Chem. **70**, 407 (2004).
[31] N. Berrah, R. C. Bilodeau, I. Dumitriu, J. D. Bozek, N. D. Gibson, C. W. Walter, G. D. Ackerman, O. Zatsarinny, and T. W. Gorczyca, Phys. Rev. A **76**, 032713 (2007).
[32] V. T. Davis, J. Thompson, and A. Covington, Nucl. Instrum. Methods Phys. Res. B **241**, 118 (2005), and references therein.
[33] S. M. O'Malley and D. R. Beck, Bull. Am. Phys. Soc. **52**, 153 (2007); and (personal communication).
[34] D. J. Pegg, Radiat. Phys. Chem. **70**, 371 (2004), and references therein.
[35] A. Osterwalder, M. J. Nee, J. Zhou, and D. M. Neumark, J. Chem. Phys. **121**, 6317 (2004).